NEOPLASIA
www.neoplasia.com

Volume 14 Number 12 December 2012 pp. 1269–1277 1269

$p16^{INK4A}$ Represses Breast Stromal Fibroblasts Migration/Invasion and Their VEGF-A–dependent Promotion of Angiogenesis through Akt Inhibition[1]

Mysoon M. Al-Ansari*, Siti-Fauziah Hendrayani*, Asma Tulbah†, Taher Al-Tweigeri‡, Afaf I. Shehata§ and Abdelilah Aboussekhra*

*Department of Molecular Oncology, King Faisal Specialist Hospital and Research Center, Riyadh, Saudi Arabia; †Department of Pathology, King Faisal Specialist Hospital and Research Center, Riyadh, Saudi Arabia; ‡Department of Oncology, King Faisal Specialist Hospital and Research Center, Riyadh, Saudi Arabia; §Department of Microbiology, King Saud University, Riyadh, Saudi Arabia

Abstract

Stromal fibroblasts, the most abundant and probably the most active cellular component of breast cancer–associated stroma, become active and promote angiogenesis through paracrine effects. However, it still unclear how these processes are regulated. Here, we have shown that down-regulation of the tumor suppressor $p16^{INK4A}$ protein enhances the migration/invasion abilities of breast stromal fibroblasts, which form dendritic network of extensions into matrigel. Furthermore, we present clear evidence that $p16^{INK4A}$ represses the expression/secretion of the proangiogenesis protein vascular endothelial growth factor A (VEGF-A). Consequently, $p16^{INK4A}$-deficient breast stromal fibroblasts and mouse embryonic fibroblasts enhanced endothelial cell differentiation into capillary-like structures in a paracrine manner. This effect was suppressed by adding bevacizumab, a specific VEGF-A inhibitor. Additionally, $p16^{INK4A}$-defective mouse embryonic fibroblasts enhanced angiogenesis in breast cancer xenografts in mice. Furthermore, we have shown that $p16^{INK4A}$ suppresses the Akt/mammalian target of rapamycin (mTOR) signaling pathway and its downstream effector hypoxia-inducible factor 1-alpha (HIF-1α), which transactivates VEGF-A. Consequently, Akt inactivation suppressed both the $p16^{INK4A}$-dependent autocrine effect on fibroblast migration/invasion and the paracrine effect on angiogenesis, showing the important role of this protein kinase in mediating the various effects related to $p16^{INK4A}$ deficiency. These results indicate that $p16^{INK4A}$ is an efficient inhibitor of the migration/invasion abilities of breast stromal fibroblasts and also their paracrine proangiogenic effects, through inhibition of Akt. Therefore, pharmacologic restoration of $p16^{INK4A}$ level in stromal fibroblasts may be exploited as therapeutic strategy to help eradicate tumor cells and/or prevent their recurrence, through suppressing cell non-autonomous procarcinogenic mediators.

Neoplasia (2012) 14, 1269–1277

Introduction

Cancer-associated fibroblasts, which constitute the major component of tumor stroma, play crucial roles in tumor onset and progression [1–3]. It has been shown that stromal fibroblasts present in invasive human breast carcinomas promote tumor growth through elevated SDF1 secretion and stimulation of tumor angiogenesis [4]. This process enables the growth of new blood vessels from adjacent microvessels, which provide nutrition and oxygen to the growing tumor allowing its growth and expansion. One key mediator of this important cancer-promoting process is the vascular endothelial growth factor A (VEGF-A) [5,6]. In a recent study, it has been shown that

Address all correspondence to: Abdelilah Aboussekhra, PhD, Molecular Oncology Department, King Faisal Specialist Hospital and Research Center, MBC #03-66, PO Box 3354, Riyadh 11211, Saudi Arabia. E-mail: aboussekhra@kfshrc.edu.sa

[1]This work was performed under Research Advisory Council (RAC) proposal No. 2080009 and was supported by King Abdelaziz City for Science and Technology (KACST) grant, under the National Comprehensive Plan for Science and Technology (KACST#08-MED480-20). The authors declare no conflict of interest.
Received 29 September 2012; Revised 24 October 2012; Accepted 29 October 2012

DOI 10.1593/neo.121632

VEGF-A secreted by reactive mouse mammary gland stromal cells enhances angiogenesis in xenografted human breast tumors [7]. Interestingly, the VEGF-A cytosolic levels in tumor tissue samples have been shown to be indicative of prognosis for patients with node-negative breast carcinoma [8]. It is noteworthy that this gene is tightly regulated at both transcriptional and post-transcriptional levels and that the Akt pathway plays a major role in this regulation [9–12].

$p16^{INK4A}$ (hereafter referred to as p16) is a cyclin-dependent kinase (CDK) inhibitor that plays multiple biologic functions, including the inhibition of cell cycle progression [13], the modulation of DNA damage–induced apoptosis [14], and the induction of senescence [15,16]. *CDKN2A* is an important tumor suppressor gene, which is frequently inactivated by point mutations, promoter methylation, or deletion in virtually all types of human cancers, including breast carcinomas [17–19]. Notably, p16-related tumor suppressor functions have been extensively studied in tumor cells, paying only little attention to its potential cell non-autonomous effects from the surrounding stromal cells, including fibroblasts. Importantly, we have recently shown that p16 is downregulated in most breast cancer–associated fibroblasts and has also cell non-autonomous tumor suppressor function [20].

In the present report, we present clear evidence that p16 downregulation enhances the migration/invasion of stromal fibroblasts and their paracrine VEGF-A–dependent angiogenesis through activation of the Akt protein kinase.

Materials and Methods

Cells, Cell Culture, and Chemicals

Breast cancer associated fibroblast 64 (CAF-64) and tumor counterpart fibroblast 64 (TCF-64) cells were obtained and cultured as previously described [21] and were always cultured simultaneously in the same conditions and at similar passages (4–8). Mouse embryonic fibroblast (MEF) cell lines (a generous gift from Dr R. A. DePinho) were cultured as previously described [22]. Human umbilical vein endothelial cells (HUVECs) and MDA-MB-231 were obtained from ATCC (Manassas, VA) and were cultured following the instructions of the company. U2OS and EH1 (a generous gift from Dr G. Peters) were cultured as previously described [23]. All supplements were obtained from Sigma (St Louis, MO) except for antibiotic and antimycotic solutions, which were obtained from Gibco (Grand Island, NY). Akt inhibitor III (Calbiochem, Rockland, MA) was dissolved in DMSO.

Cellular Lysate Preparation and Immunoblot Analysis

This has been performed as previously described [23]. Antibodies directed against Akt, phospho-Akt (193H12), mammalian target of rapamycin (mTOR, 7C10), and p.mTOR (Ser2448, D9C2) were purchased from Cell Signaling Technology (Danvers, MA), VEGF-A from Abcam (Cambridge, MA), p16 and CD31 from BD Biosciences (San Jose, CA), glyceraldehyde 3-phosphate dehydrogenase (GAPDH, FL-335) from Santa Cruz Biotechnology (Santa Cruz, CA), and HIF-1α (H1α67) from Millipore (Rockland, MA).

RNA Purification, Reverse Transcription–Polymerase Chain Reaction, and Real-time Reverse Transcription–Polymerase Chain Reaction

This has been performed as previously described [20].

The respective primers were:

β-actin: 5′-CCCAGCACAATGAAGATCAAGATCAT-3′ and 5′ ATCTGCTGGAAGGTGGACAGCGA-3′;

CDKN2A: 5′-CAACGCACCGAATAGTTACG-3′ and 5′-CAGCTCCTCAGCCAGGTC-3′

VEGF-A: 5′-CCCACTGAGGAGTCCAACAT-3′ and 5′-TTTCTTGCGCTTTCGTTTTT-3′.

siRNA Transfection

The transfection using *CDKN2A*-siRNA and control-siRNA was performed as previously described [23]. The *AKT*-siRNA and its corresponding control were obtained from Qiagen (Hilden, Germany), and the transfections were carried out as recommended by the manufacturer.

Viral Infection

Lentivirus-based vector bearing *CDKN2A*-ORF (pIRES) as well as its respective control (Addgene, Cambridge, MA) were used to prepare the lentiviral supernatant from 293FT cells. Lentiviral supernatants were collected 48 hours post-transfection, filtered, and used for infection. Twenty-four hours later, media were replaced with complete media (CpM) and cells were grown for 3 days.

Enzyme-linked Immunosorbent Assay

Supernatants from 24-hour fibroblast cell cultures were harvested and ELISA was performed according to the manufacturer's instructions [R&D Systems (Minneapolis, MN) or Ray Bio (Brussels, Belgium) for MMP-2]. The OD was used at 450 nm on a standard ELISA plate reader. These experiments were performed in triplicates.

Chemotaxis and Invasion Assay

Cell migration and invasion were evaluated using 24-well BD BioCoat Matrigel Invasion Chambers as per the manufacturer guideline (BD Biosciences). In brief, 2 to 4×10^5 cells were added to the upper wells separated by 0.8-μm pore-size polyethylene terephthalate (PET) membrane with thin layer of matrigel basement membrane matrix (for invasion) or without (for migration). The membranes were stained with Diff-Quick stain (Fisher Scientific, Fair Lawn, NJ) after removing the non-migrated cells from the top of the membrane with Q-tips. After air-drying, the membranes were cut and mounted on slides with oil, and cells that had migrated to the underside of the filter were counted using light microscope (Zeiss Axio Observer) in five randomly selected fields (original magnification, ×40). Each assay was performed in triplicate.

Three-dimensional Matrigel Assay

Fibroblast cells (6×10^4) were seeded in the presence of CpM in 6-well plates coated with solidified BD Matrigel basement membrane matrix. After 24 hours of incubation, cells were photographed.

Quantification of Protein and RNA Expression Levels

The expression levels of the immunoblotted proteins were measured using a densitometer (BIO-RAD GS-800 Calibrated Densitometer), as previously described [23].

HUVEC Endothelial Tube Formation Assay

The Chemicon *In Vitro* Angiogenesis Assay Kit was used. Wells in 96-well plates were coated with ice-cold EC matrix gel solution in the EC matrix diluent buffer. After solidification of the matrix at 37°C, 5000 HUVECs were seeded onto the polymerized EC matrix in the presence of 150 μl of RPMI per well. Media were immediately added after plating HUVECs for a final 1:1 ratio of RPMI medium to

conditioned media. After 4 hours of incubation, tubule branches were photographed and their number was counted.

Conditioned Media

Cells were cultured in medium ± serum for 24 hours, and then media were collected and briefly centrifuged. The resulting supernatants were used either immediately or were frozen at −80°C until needed.

Tumor Xenografts

Animal experiments were approved by the King Faisal Specialist Hospital and Research Center Institutional Animal Care and Use Committee and were conducted according to relevant national and international guidelines. Animals were housed in the King Faisal Specialist Hospital and Research Center animal facility and they only suffered needle injection pain and also certain degree of pain/distress related to the growth/burden of the tumor. The euthanasia was performed using CO_2 chamber and cervical dislocation. Ten nude mice were randomized into two groups, and breast cancer xenografts were created by subcutaneous coimplantation of MDA-MB-231 cells (2×10^6) with p16−/− or p16+/+ MEFs (10^6) into the right leg of each mouse. After 49 days, the animals were scarified and tumors were excised.

Evaluation of Microvessel Density in Tumor Xenografts

Paraffin-embedded sections from tumor xenografts were immunostained using anti-CD31 antibody, and then the number of CD31-positive vessels was counted in five different highest fields of microvessel density (40× objective lens and 10× ocular lens).

Statistical Analysis

Statistical analysis was performed by Student's *t* test and *P* values of .05 and less were considered as statistically significant.

Results

p16 Represses Stromal Fibroblast Migration and Invasion

We have shown in a recent publication that p16 down-regulation activates breast stromal fibroblasts [20]. Therefore, we sought to investigate whether p16 plays a role in stromal fibroblast migration and invasion, two major features of active fibroblasts. To this end, we down-regulated p16 in histologically normal TCF-64 cells using specific

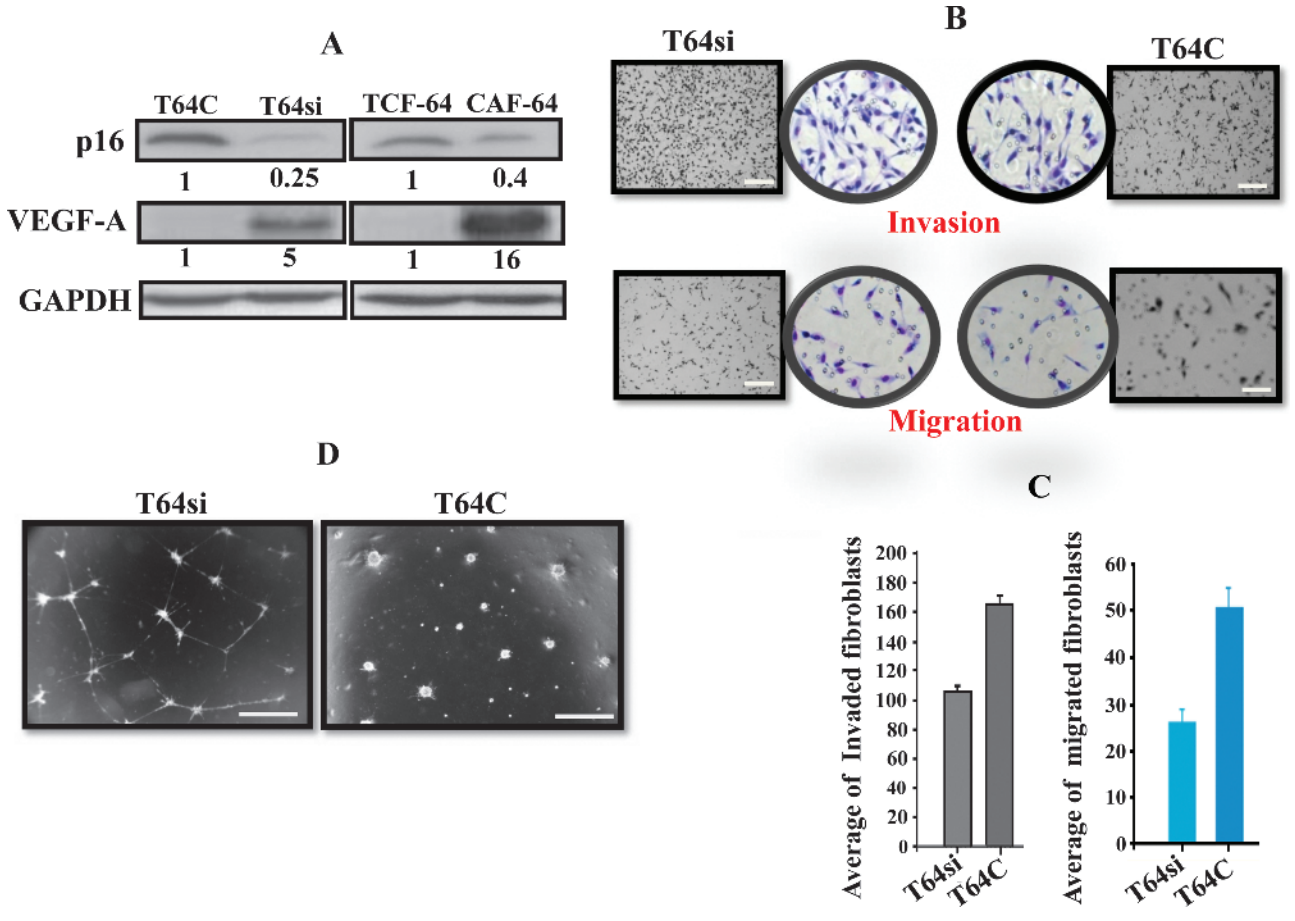

Figure 1. p16 down-regulation enhances fibroblast migration and invasion. (A) Whole-cell lysates were prepared from TCF-64, CAF-64, T64si, and T64C cells and were used for immunoblot analysis. The numbers below the bands indicate fold of induction after normalization against GAPDH. (B, C) T64si and T64C cells (4×10^5) were cultured on the upper compartments of BioCoat Matrigel chambers in the presence of SFM. After 24 hours of incubation, cells were stained with Diff-Quick stain and then counted. (B) Representative photographs showing invasive and migrated cells. Scale bars represent 20 μm. (C) Histograms depict average numbers of invasive and migrated cells, and error bars represent means ± SD. (D) Cells (6×10^4) were seeded with CpM in six-well plates coated with BD Matrigel basement membrane matrix for 24 hours. Representative photographs show the morphology of the invading cells. Scale bars represent 30 μm.

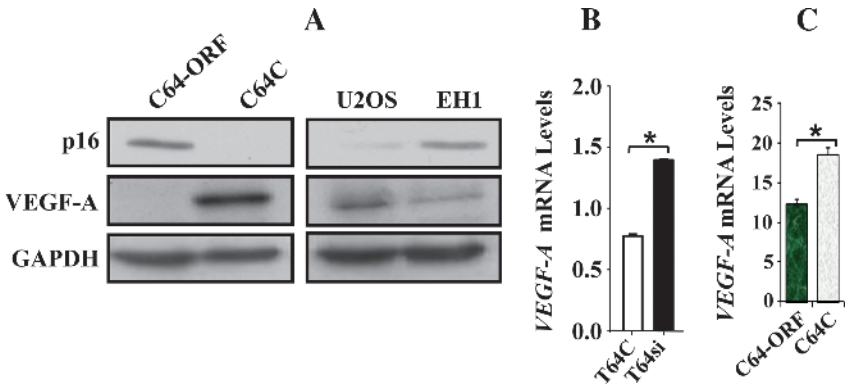

Figure 2. p16 suppresses the expression of VEGF-A. (A) Cell lysates were prepared from the indicated cells and used for immunoblot analysis using the indicated antibodies. (B, C) Total RNA was extracted from the indicated cells and the amount of the *VEGF-A* mRNA was assessed by real-time RT-PCR. Error bars represent means ± SD. *$P < .001$.

siRNA (T64si), and scrambled siRNA was used as control (T64C). T64si and T64C cells had similar growth rate and were always treated simultaneously. Cell lysates were prepared from these cells and from TCF-64 and the corresponding CAF-64 cells, and the p16 protein levels were assessed by immunoblot analysis. Figure 1*A* shows p16 down-regulation by *CDKN2A*-siRNA–expressing cells. It is noteworthy that the expression of p14 was not affected in these cells [20]. Next, we assessed the migratory/invasiveness abilities of T64si and T64C cells using BioCoat Matrigel chambers either coated (invasion) or uncoated (migration). While CpM was added as chemoattractant to the lower wells of the chambers, cells (4×10^5) were added to the upper wells in the presence of serum-free media (SFM). After 24 hours of incubation, cells were stained with Diff-Quick stain and then counted. Figure 1, *B* and *C*, shows that the number of migrating and invading p16-deficient cells was about two-fold higher than the number of migrating ($P = .00011$) and invading ($P = .0000035$) control cells. This suggests that p16 represses both the migratory and the invasiveness abilities of breast stromal fibroblast cells.

We next investigated the role of p16 in the migration/invasion of breast fibroblasts in *in vitro* three-dimensional (3D) matrigel assay. Thereby, T64si and T64C cells (6×10^4) were embedded in the BD Matrigel. While all cells formed spheroids in the matrigel, only the p16-deficient fibroblasts showed invasive growth in a stellate pattern with branching morphogenesis forming dendritic network of extensions (Figure 1*D*). This shows that p16 down-regulation changes the 3D shape and enhances the invasiveness of breast stromal fibroblasts into matrigel.

p16 Negatively Regulates VEGF-A Expression in Breast Stromal Fibroblasts

Because CAFs play a major role in angiogenesis and because the increase in the migratory ability of stromal fibroblasts and their branching structure is thought to help the formation of new blood vessels [24], we sought to investigate the possible role of p16 in the expression of the main angiogenesis factor VEGF-A in stromal fibroblasts and the paracrine effect on endothelial cells. To this end, the level of VEGF-A was assessed in T64si and T64C cells. Figure 1*A* shows clear increase (five-fold) in the level of VEGF-A in p16-deficient cells compared to control cells. Similarly, the VEGF-A level is 16-fold higher in CAF-64 cells than in the corresponding TCF-64 cells (Figure 1*A*). In addition, CAF-64 cells were transfected with lentivirus-based plasmids expressing *CDKN2A* (C64-ORF) or not (C64C), and then the level of the VEGF-A protein was assessed. Figure 2*A* shows that the introduction of the *CDKN2A*-ORF in CAF-64 cells increased the level of p16 and concomitantly reduced the expression of VEGF-A. Similarly, the expression of p16 in the p16-defectrive osteosarcoma U2OS cells (EH1) reduced the expression level of VEGF-A (Figure 2*A*). EH1 expresses p16 under the control of an isopropyl β-D-1-thiogalactopyranoside (IPTG)–inducible promoter, but in absence of IPTG there is a leaky expression, which does not exert any measurable effect on cellular growth [25]. These results suggest that p16 represses the expression of VEGF-A.

To investigate the effect of p16 on the VEGF-A mRNA, total RNA was purified from T64C and T64si cells, and real-time reverse transcription–polymerase chain reaction (RT-PCR) using specific primers was performed. Figure 2*B* shows that the mRNA level of *VEGF-A* doubled in T64si cells compared to the control T64C ($P = .00082$), indicating that the *VEGF-A* mRNA expression is modulated in a p16-dependent manner. To further show this, total RNA was purified from C64-ORF and C64C cells and real-time

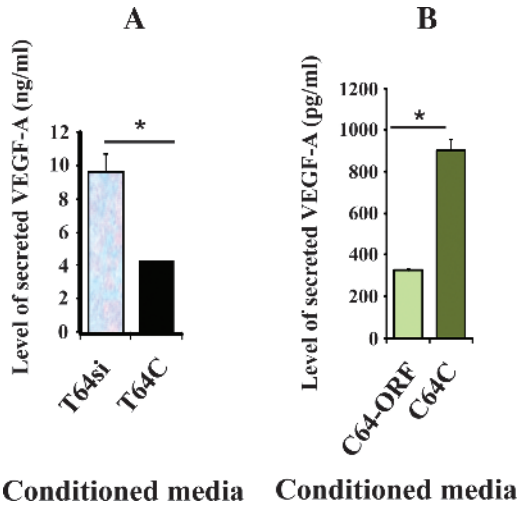

Figure 3. p16 represses VEGF-A secretion from breast stromal fibroblasts. (A, B) Conditioned media from the indicated cells were collected after 24 hours and the level of secreted VEGF-A was determined by ELISA. Error bars represent means ± SD. *$P < .001$.

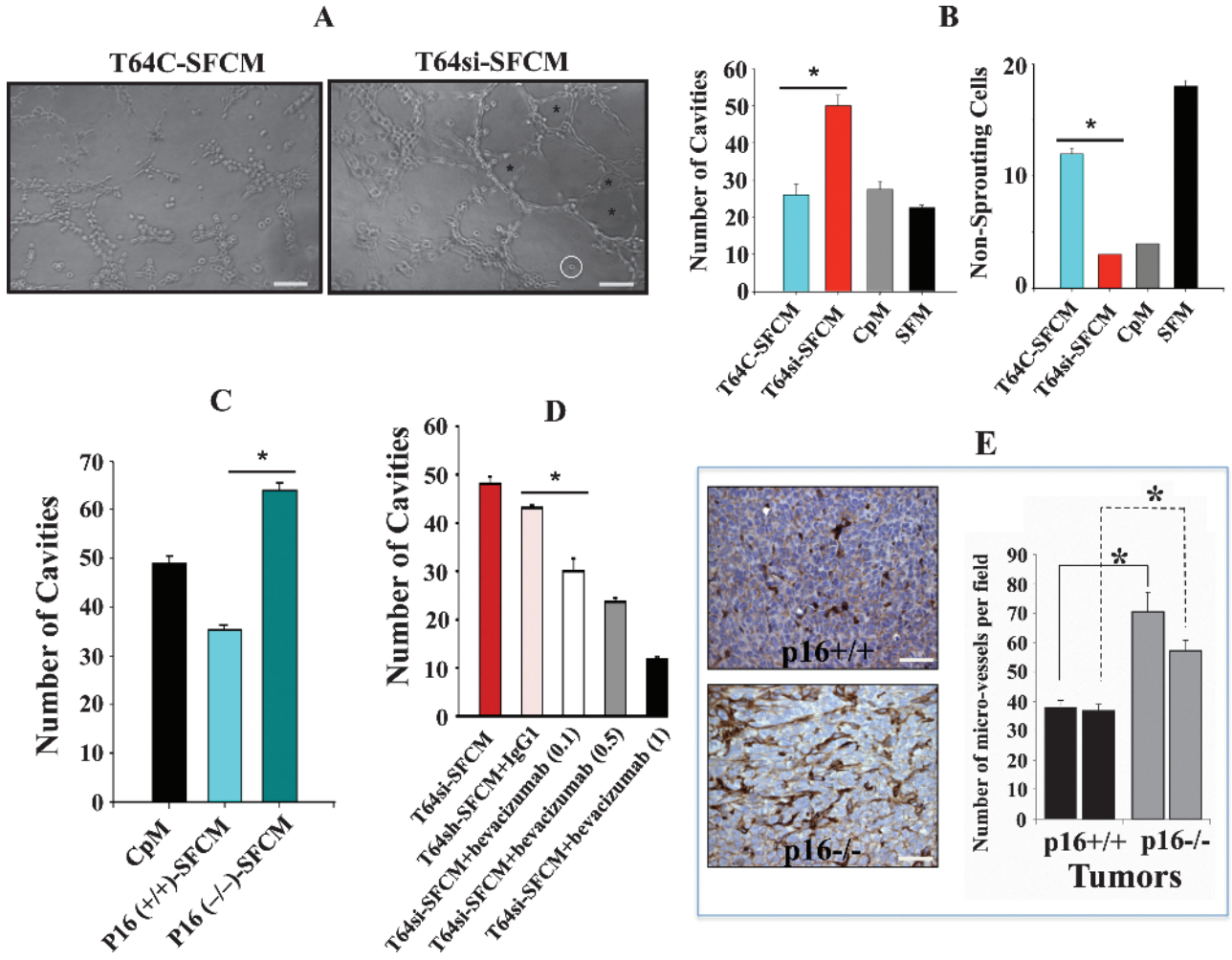

Figure 4. SFCM from p16-deficient human and mice fibroblasts activate HUVEC tube formation in a VEGF-A–dependent manner. SFCM were collected after 24 hours of incubation from the indicated cells and were added independently on HUVECs plated on matrigel (96-well plate), and the differentiation into capillary-like structures was assessed after 4 hours of incubation. (A) Representative photographs of HUVEC cavities. Scale bars represent 30 μm. Stars show cavities and the circle indicates non-sprouting cells. (B) Histograms show number of cavities and non-sprouting cells. (C) SFCM were collected from MEF cells. (D) SFCM from T64si cells were treated with IgG1 or bevacizumab. The numbers between brackets indicate bevacizumab concentrations in μM. (E) Breast cancer xenografts were created by co-injecting MDA-MB-231 cells with p16−/− or p16+/+ MEFs subcutaneously into nude mice. Immunohistochemistry was carried out on tumors containing MEFs either p16−/− or p16+/+ using anti–CD-31 antibody. Scale bars represent 30 μm. Histogram shows average number of microvessels observed in five different fields from two different tumors. Error bars represent means ± SD. *$P < .001$.

RT-PCR was performed. Figure 2*C*, *upper panel*, shows clear increase in the level of *CDKN2A* in cells expressing the gene. The lower panel shows that the introduction of the *CDKN2A*-ORF in CAF-64 cells significantly reduced the expression of the VEGF-A mRNA (P = .000742). This confirms the p16-dependent expression of the *VEGF-A* gene.

p16 Suppresses the Secretion of VEGF-A from Breast Stromal Fibroblasts

T64si and T64C cells were cultured in CpM for 24 hours, and conditioned medium from each culture was collected and was used to assess the level of secreted VEGF-A by ELISA. Figure 3*A* shows that down-regulation of p16 significantly increased the secreted level of VEGF-A (about three-fold). Furthermore, conditioned media from C64-ORF and C64C cells were collected and the level of VEGF-A was assessed by ELISA. Figure 3*B* shows that the increase in the level of the p16 coding gene significantly reduced the secreted level of VEGF-A. This indicates that p16 restrains the secretion of this angiogenesis-promoting protein from breast stromal fibroblasts.

Breast Stromal Fibroblast p16 Suppresses Angiogenesis

SFM were conditioned with T64si and T64C cells for 24 hours and were subsequently added separately to 96-well plates seeded with 0.5×10^5 HUVECs in matrigel and used for *in vitro* angiogenic assay. SFM was also added as negative control. Figure 4*A* shows that after 4 hours of incubation the number of HUVECs that were differentiated into closed cavity constructions was significantly higher in the presence of serum-free conditioned media (SFCM) from T64si cells compared to SFCM from T64C cells or SFM, with a P value of .0000464. Similarly, the number of non-sprouting HUVECs was 4-fold and 4.5-fold lower in the presence of SFCM derived from p16-deficient cells compared to p16-proficient cells (P = .0000357)

and SFM, respectively (Figure 4*B*). Similar results were obtained with MEF-p16–/– SFCM compared to MEF-p16+/+ SFCM (Figure 4*C*). These results illustrate the role of the stromal fibroblast p16 protein in inhibiting endothelial cell differentiation into capillary-like structures through paracrine effect.

To ascertain the role of stromal fibroblast–secreted VEGF-A in the differentiation of HUVECs, SFCM from T64si cells were treated with IgG1 (control) or increasing concentrations of the anti–VEGF-A inhibitory antibody bevacizumab. Figure 4*D* shows that the number of HUVECs that were differentiated into closed cavity constructions decreased in a dose-dependent manner. In response to 1 μM bevacizumab, only 25% of the cavities were formed compared to the control cells treated with IgG1 (Figure 4*D*). This shows that p16-deficient stromal fibroblast-dependent activation of HUVEC differentiation is indeed VEGF-A related.

To investigate the effect of p16 deficiency in fibroblasts on angiogenesis *in vivo*, 10 nude mice were randomized into two groups and breast cancer xenografts were created subcutaneously by coimplantation of MDA-MB-231 cells (2×10^6) with p16–/– or p16+/+ MEFs (10^6) into the right leg of each mouse. After the formation of the tumors, we examined the paracrine effect of p16 on vascular formation in tumor xenografts by immunohistochemistry using anti-CD31 antibody, an endothelial cell marker. Figure 4*E* shows higher density of CD31-positive vessels in tumors containing MEF-p16–/– cells compared to xenograft tumors admixed with normal MEFs. Interestingly, the assessment of the averaged microvascular density in both tumor xenografts showed two-fold greater level in tumors containing MEF-p16–/– when compared with tumors containing normal counterpart MEF cells (Figure 4*E*). This further shows the antiangiogenesis role of stromal fibroblast p16.

p16 Inhibits the Akt/mTOR Pathway

To explore the molecular mechanisms that underlay p16-dependent modulation in stromal fibroblast migration/invasion and their proangiogenic effects, we studied the effect of *CDKN2A* down-regulation on the phosphorylation/activation of Akt, a known proinvasive and proangiogenesis protein kinase [9,26]. Figure 5*A* shows that while the level of Akt was not affected with p16 knockdown, the level of the active form of the protein was upregulated in p16-deficient cells compared to their control cells. To further elucidate the role of p16 in Akt inhibition, we checked the status of Akt in CAF-64 cells expressing the *CDKN2A* gene and their respective control cells. Figure 5*B* shows that p16 expression in CAF-64 reduced the level of the active form of the Akt protein kinase. Similarly, while p16-defective U2OS cells express high level of the phosphorylated Akt protein, the isogenic p16-proficient EH1 cells express only a low amount of the active Akt (Figure 5*B*). This indicates that p16 inhibits Akt, which could explain the increase in the migration/invasion ability of p16-deficient breast stromal fibroblasts.

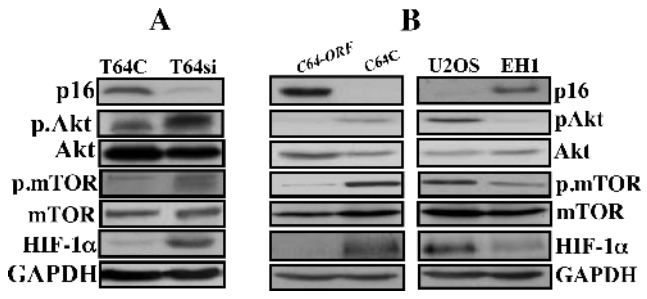

Figure 5. p16 represses the Akt/mTOR/HIF-1α pathway. (A, B) Whole-cell lysates were prepared from the indicated cells and were used for immunoblot analysis using the indicated antibodies.

Active Akt induces angiogenesis through the activation of the mTOR and HIF-1α genes [27]. To test this, we assessed the levels of these proteins in p16-deficient cells compared to their control counterparts. Figure 5*A* shows that the activation of Akt in p16-deficient cells was accompanied by activation of the mTOR protein and the up-regulation of its major target HIF-1α, which is a positive regulator of VEGF-A and angiogenesis [28]. However, p16 expression in p16-deficient CAF-64 and U2OS cells reduced the level of the active mTOR and its downstream effector HIF-1α (Figure 5*B*). This confirms the role of p16 deficiency in the activation of the Akt pathway.

p16 Represses Stromal Fibroblasts Migration and Their Proangiogenic Effect through Inhibiting the Akt Pathway

To confirm the role of Akt in mediating p16 deficiency–related enhancement of stromal fibroblast migration/invasion and angiogenesis, we inhibited this kinase in T64si using both Akt inhibitor III at 10 μM for 18 hours and a specific Akt-siRNA. At this concentration, Akt inhibitor III had no effect on cell proliferation or cytotoxicity. Figure 6*A* shows the inhibitory effect of the Akt inhibitor and Akt-siRNA on the expression level of Akt and phopho-Akt. As expected, while inhibitor III affected the level of the active form of the protein, Akt-siRNA reduced the level of both total and phospho-Akt (Figure 6*A*). Next, we investigated the effect of Akt inhibition on invasion/migration as described in Figure 1*B*. Interestingly, Akt inhibition strongly reduced the migratory and invasiveness abilities of p16-deficient stromal fibroblasts (Figure 6, *B* and *C*). Similarly, Akt inhibitor III suppressed the invasive growth of these cells into matrigel compared to their control counterpart cells (Figure 6*D*). This indicates that the p16-related increase in the migration/invasion abilities of breast stromal fibroblasts is Akt-dependent.

To assess the effect on angiogenesis, SFM conditioned with T64si cells pretreated with DMSO or Akt inhibitor III were collected and were added to HUVECs as described in Figure 4*A*. Figure 6*E* shows that after 4 hours of incubation in the presence of SFCM from control cells, HUVECs were differentiated into closed cavities. However, no differentiation was observed in the presence of SFCM from Akt inhibitor–treated cells. Similar effects were obtained when Akt was inhibited by specific siRNA (data not shown), showing that p16 inhibits the proangiogenic effect of stromal fibroblasts by suppressing the Akt pathway.

Discussion

When active, CAFs become more invasive and prepare the milieu for cancer spread through activating neovascularization in a paracrine manner [4,29]. Both cancer epithelial cells and stromal fibroblasts are interdependent for their migratory behavior through cross-signaling; however, it still unclear which cell population starts invading the other one. To do so, active stromal fibroblasts need to traverse the extracellular matrix and the basement membrane. We have shown here that p16 down-regulation enhances the migratory and the invasiveness abilities of mammary stromal fibroblasts. Furthermore, p16 down-regulation changed also the 3D structure of breast

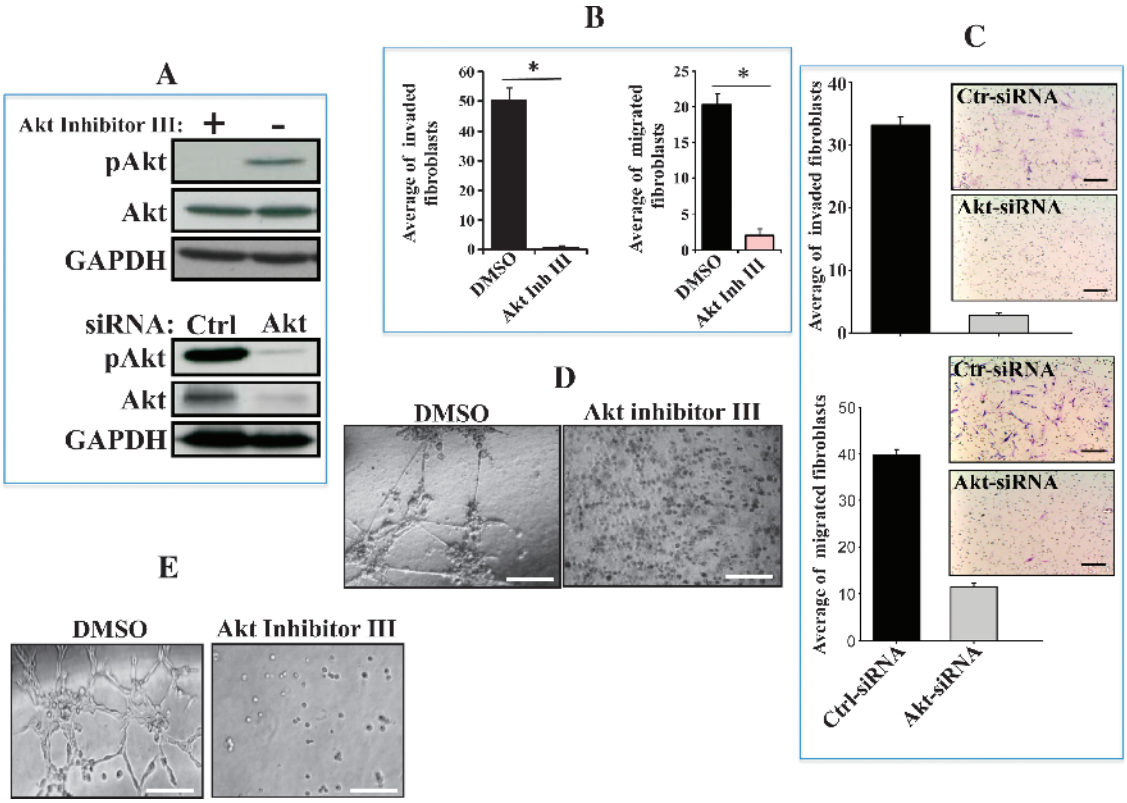

Figure 6. p16 represses stromal fibroblasts migration/invasion and their proangiogenic effect through Akt inhibition. (A) T64si cells were treated with Akt inhibitor III (10 μM) and DMSO (−) for 18 hours (upper panel) or cells were treated with control-siRNA and Akt-siRNA (lower panel), and whole-cell lysates were prepared and used for immunoblot analysis using the indicated antibodies. (B, D, E) T64si cells were treated either with Akt inhibitor III (10 μM) or DMSO. (B, D) The migration and invasion abilities were assessed using matrigel chambers as in Figure 1*C*. Error bars represent means ± SD. *$P < .001$ (B), or BD matrigel basement membrane matrix as in Figure 1*D* (D). (C) T64si cells were treated either with control-siRNA or Akt-siRNA, and the migration/invasion abilities of these cells were assessed as in Figure 1*C*. Representative photographs of migrating and invading cells are shown. Error bars represent means ± SD. (E) SFCM were collected and were added independently on HUVECs plated on matrigel (96-well plate), and the differentiation into capillary-like structures was assessed after 4 hours of incubation. Representative photographs of HUVEC cavities are shown. Scale bars represent 30 μm.

fibroblasts by triggering the formation of branching structures with dendritic network of extensions and also increased their invasiveness into matrigel, which is an *in vitro* mimic of the basement membrane (Figure 1). This reveals that p16 repression may be critical in increasing the ability of stromal fibroblasts in moving and invading the epithelial compartment. During mammary carcinogenesis, this could constitute an important step toward the transition from ductal carcinoma *in situ* (DCIS) to invasive ductal carcinoma, because the basement membrane is largely intact in ductal carcinoma *in situ*. Besides, these branching structures of activated fibroblasts could also increase the efficiency of stromal fibroblasts in recruiting endothelial progenitor cells and the formation of blood vessels. Indeed, we have also shown that p16-deficient fibroblasts express and secrete higher levels of the proangiogenesis factor VEGF-A and enhance endothelial cell differentiation into capillary-like structures and angiogenesis *in vivo* in breast tumor xenografts.

In a previous study, Li et al. have shown that adenoviral-mediated p16 expression downregulated the VEGF-A gene expression in breast cancer cells and suppressed breast cancer cell–induced angiogenesis [30]. Similarly, restoration of p16 reduced the VEGF-A expression level and inhibited angiogenesis in human gliomas [31]. In the present study, we have shown that p16 represses the VEGF-A expression at both mRNA and protein levels in breast fibroblasts. Indeed, while p16 down-regulation increased the VEGF-A mRNA and protein levels, p16 expression decreased the level of the VEGF-A mRNA, suggesting that p16 controls the expression of VEGF-A at the transcriptional or post-transcriptional level.

These results raised an important question regarding how p16 controls these two important cancer-promoting processes: fibroblast migratory ability and the synthesis/secretion of the proangiogenic factor VEGF-A. Interestingly, both of these processes are under the control of the important protein kinase Akt [32]. We have shown that p16 negatively controls Akt, and the inhibition of this kinase suppressed the migration/invasion abilities of p16-deficient stromal fibroblasts and also their paracrine proangiogenesis effect.

To elucidate the molecular pathway underlying the p16-dependent repression of the VEGF-A expression, we tested the effect of p16 down-regulation on HIF-1α, the major transcriptional activator of VEGF-A, which is also under the control of the Akt/mTOR pathway [33]. Interestingly, we have found the *HIF-1α* gene upregulated in p16-deficient cells. This suggests that p16 negatively regulates VEGF-A through inhibition of HIF-1α. This effect seems to take place through the inhibition of the Akt/mTOR pathway. Indeed, p16 down-regulation activated mTOR (Figure 5).

How does p16 regulate the activity/expression of these genes? In fact, several lines of evidence indicate that p16 is not a mere CDK inhibitor. p16 overexpression has also been found in some benign tumors and in some cancer types, such as cervical cancer, breast cancer, and head and neck cancer [34,35]. Therefore, it is possible that this p16 function is mediated through interaction with other proteins. Indeed, it has been shown that p16 interacts with several proteins involved directly or indirectly in the control of gene expression such as HSP90, EF-2, hnRNP C1, and others [36]. Furthermore, it has been recently shown that p16 interacts with GRAM-19 to regulate E2F1-responsive gene expression [37]. Moreover, p16 down-regulation by specific siRNA modulated the expression of more than 2000 genes implicated in different cellular processes [38]. Additionally, Chien et al. have shown the implication of p16 in controlling the expression of several miRNA in cancer cells [39]. This indicates that p16 may regulate gene expression at different levels through protein-protein interactions and modulating the expression of various key transcription factors.

The fact that p16 represses both migration/invasion of breast stromal fibroblasts and their proangiogenic effect indicates that the loss of this tumor suppressor gene plays a major role in the activation of these cells and consequently in tumor growth and spread. We have recently shown that p16 is downregulated in 83% breast CAFs compared to their adjacent counterpart primary cells and also in breast cancer tissues *in situ*. Furthermore, specific p16 down-regulation enhanced the procarcinogenic effects of breast stromal fibroblasts both *in vitro* and in tumor xenografts [20]. Additionally, p16 promoter hypermethylation and transcriptional silencing have been detected in histologically normal mammary tissue of cancer-free women. This led to COX-2 overexpression and promotion of premalignant program, including increased angiogenic activity [40,41]. This shows that loss of p16 function promotes tumorigenesis and angiogenesis not only from cancer cells [30,31] but also from the abundant activated stromal fibroblasts in a paracrine fashion. Therefore, pharmacologic restoration of p16 level in breast stroma could be of great therapeutic value.

Acknowledgments

We thank P. Hall for critical reading of the manuscript. We also thank the Comparative Medicine staff for their help with animals.

References

[1] Aboussekhra A (2011). Role of cancer-associated fibroblasts in breast cancer development and prognosis. *Int J Dev Biol* **55**, 841–849.

[2] Shimoda M, Mellody KT, and Orimo A (2009). Carcinoma-associated fibroblasts are a rate-limiting determinant for tumour progression. *Semin Cell Dev Biol* **21**, 19–25.

[3] Franco OE, Shaw AK, Strand DW, and Hayward SW (2009). Cancer associated fibroblasts in cancer pathogenesis. *Semin Cell Dev Biol* **21**, 33–39.

[4] Orimo A, Gupta PB, Sgroi DC, Arenzana-Seisdedos F, Delaunay T, Naeem R, Carey VJ, Richardson AL, and Weinberg RA (2005). Stromal fibroblasts present in invasive human breast carcinomas promote tumor growth and angiogenesis through elevated SDF-1/CXCL12 secretion. *Cell* **121**, 335–348.

[5] Bergers G and Benjamin LE (2003). Tumorigenesis and the angiogenic switch. *Nat Rev Cancer* **3**, 401–410.

[6] Carmeliet P (2005). VEGF as a key mediator of angiogenesis in cancer. *Oncology* **69**(suppl 3), 4–10.

[7] Pinto MP, Badtke MM, Dudevoir ML, Harrell JC, Jacobsen BM, and Horwitz KB (2010). Vascular endothelial growth factor secreted by activated stroma enhances angiogenesis and hormone-independent growth of estrogen receptor-positive breast cancer. *Cancer Res* **70**, 2655–2664.

[8] Gasparini G, Toi M, Gion M, Verderio P, Dittadi R, Hanatani M, Matsubara I, Vinante O, Bonoldi E, Boracchi P, et al. (1997). Prognostic significance of vascular endothelial growth factor protein in node-negative breast carcinoma. *J Natl Cancer Inst* **89**, 139–147.

[9] Jiang BH and Liu LZ (2008). AKT signaling in regulating angiogenesis. *Curr Cancer Drug Targets* **8**, 19–26.

[10] Xin H, Brown JA, Gong C, Fan H, Brewer G, and Gnarra JR (2012). Association of the von Hippel-Lindau protein with AUF1 and posttranscriptional regulation of VEGFA mRNA. *Mol Cancer Res* **10**, 108–120.

[11] Merdzhanova G, Gout S, Keramidas M, Edmond V, Coll JL, Brambilla C, Brambilla E, Gazzeri S, and Eymin B (2010). The transcription factor E2F1 and the SR protein SC35 control the ratio of pro-angiogenic versus antiangiogenic isoforms of vascular endothelial growth factor-A to inhibit neovascularization *in vivo*. *Oncogene* **29**, 5392–5403.

[12] Essafi-Benkhadir K, Onesto C, Stebe E, Moroni C, and Pages G (2007). Tristetraprolin inhibits Ras-dependent tumor vascularization by inducing vascular endothelial growth factor mRNA degradation. *Mol Biol Cell* **18**, 4648–4658.

[13] Okamoto K, Kamibayashi C, Serrano M, Prives C, Mumby MC, and Beach D (1996). p53-dependent association between cyclin G and the B′ subunit of protein phosphatase 2a. *Mol Cell Biol* **16**, 6593–6602.

[14] Al-Mohanna MA, Manogaran PS, Al-Mukhalafi Z, Al-Hussein AK, and Aboussekhra A (2004). The tumor suppressor $p16^{INK4a}$ gene is a regulator of apoptosis induced by ultraviolet light and cisplatin. *Oncogene* **23**, 201–212.

[15] Bae I, Smith ML, Sheikh MS, Zhan Q, Scudiero DA, Friend SH, O'Connor PM, and Fornace AJ Jr (1996). An abnormality in the p53 pathway following gamma-irradiation in many wild-type p53 human melanoma lines. *Cancer Res* **56**, 840–847.

[16] Ohtani N, Yamakoshi K, Takahashi A, and Hara E (2004). The $p16^{INK4a}$-RB pathway: molecular link between cellular senescence and tumor suppression. *J Med Invest* **51**, 146–153.

[17] Ruas M and Peters G (1998). The $p16^{INK4a}$/CDKN2A tumor suppressor and its relatives. *Biochim Biophys Acta* **1378**, F115–F177.

[18] Rocco JW and Sidransky D (2001). p16(MTS-1/CDKN2/INK4a) in cancer progression. *Exp Cell Res* **264**, 42–55.

[19] Li J, Poi MJ, and Tsai MD (2011). Regulatory mechanisms of tumor suppressor $P16^{INK4A}$ and their relevance to cancer. *Biochemistry* **50**, 5566–5582.

[20] Al-Ansari MM, Hendrayani SF, Shehata AI, and Aboussekhra A (2012). $p16^{INK4A}$ represses the paracrine tumor-promoting effects of breast stromal fibroblasts. *Oncogene*. DOI:10.1038/onc.2012.270.

[21] Hawsawi NM, Ghebeh H, Hendrayani SF, Tulbah A, Al-Eid M, Al-Tweigeri T, Ajarim D, Alaiya A, Dermime S, and Aboussekhra A (2008). Breast carcinoma-associated fibroblasts and their counterparts display neoplastic-specific changes. *Cancer Res* **68**, 2717–2725.

[22] Sharpless NE, Bardeesy N, Lee KH, Carrasco D, Castrillon DH, Aguirre AJ, Wu EA, Horner JW, and DePinho RA (2001). Loss of $p16^{Ink4a}$ with retention of $p19^{Arf}$ predisposes mice to tumorigenesis. *Nature* **413**, 86–91.

[23] Al-Mohanna MA, Al-Khalaf HH, Al-Yousef N, and Aboussekhra A (2007). The $p16^{INK4a}$ tumor suppressor controls $p21^{WAF1}$ induction in response to ultraviolet light. *Nucleic Acids Res* **35**, 223–233.

[24] Vong S and Kalluri R (2011). The role of stromal myofibroblast and extracellular matrix in tumor angiogenesis. *Genes Cancer* **2**, 1139–1145.

[25] McConnell BB, Gregory FJ, Stott FJ, Hara E, and Peters G (1999). Induced expression of $p16^{INK4a}$ inhibits both CDK4- and CDK2-associated kinase activity by reassortment of cyclin-CDK-inhibitor complexes. *Mol Cell Biol* **19**, 1981–1989.

[26] Yoeli-Lerner M, Yiu GK, Rabinovitz I, Erhardt P, Jauliac S, and Toker A (2005). Akt blocks breast cancer cell motility and invasion through the transcription factor NFAT. *Mol Cell* **20**, 539–550.

[27] Skinner HD, Zheng JZ, Fang J, Agani F, and Jiang BH (2004). Vascular endothelial growth factor transcriptional activation is mediated by hypoxia-inducible factor 1α, HDM2, and p70S6K1 in response to phosphatidylinositol 3-kinase/AKT signaling. *J Biol Chem* **279**, 45643–45651.

[28] Semenza GL (2003). Targeting HIF-1 for cancer therapy. *Nat Rev Cancer* **3**, 721–732.

[29] Allen M and Louise Jones J (2011). Jekyll and Hyde: the role of the microenvironment on the progression of cancer. *J Pathol* **223**, 162–176.

[30] Li M, Zhang Z, Hill DL, Wang H, and Zhang R (2007). Curcumin, a dietary component, has anticancer, chemosensitization, and radiosensitization effects by down-regulating the *MDM2* oncogene through the PI3K/mTOR/ETS2 pathway. *Cancer Res* **67**, 1988–1996.

[31] Harada H, Nakagawa K, Iwata S, Saito M, Kumon Y, Sakaki S, Sato K, and Hamada K (1999). Restoration of wild-type p16 down-regulates vascular

endothelial growth factor expression and inhibits angiogenesis in human gliomas. *Cancer Res* **59**, 3783–3789.

[32] Jiang BH and Liu LZ (2008). PI3K/PTEN signaling in tumorigenesis and angiogenesis. *Biochim Biophys Acta* **1784**, 150–158.

[33] Semenza GL (2010). HIF-1: upstream and downstream of cancer metabolism. *Curr Opin Genet Dev* **20**, 51–56.

[34] Romagosa C, Simonetti S, Lopez-Vicente L, Mazo A, Lleonart ME, Castellvi J, and Ramon y Cajal S (2011). $p16^{Ink4a}$ overexpression in cancer: a tumor suppressor gene associated with senescence and high-grade tumors. *Oncogene* **30**, 2087–2097.

[35] Witkiewicz AK, Knudsen KE, Dicker AP, and Knudsen ES (2011). The meaning of $p16^{ink4a}$ expression in tumors: functional significance, clinical associations and future developments. *Cell Cycle* **10**, 2497–2503.

[36] Souza-Rodrigues E, Estanyol JM, Friedrich-Heineken E, Olmedo E, Vera J, Canela N, Brun S, Agell N, Hubscher U, Bachs O, et al. (2007). Proteomic analysis of $p16^{ink4a}$-binding proteins. *Proteomics* **7**, 4102–4111.

[37] Sun P, Nallar SC, Raha A, Kalakonda S, Velalar CN, Reddy SP, and Kalvakolanu DV (2010). GRIM-19 and $p16^{INK4a}$ synergistically regulate cell cycle progression and E2F1-responsive gene expression. *J Biol Chem* **285**, 27545–27552.

[38] Al-Khalaf HH, Colak D, Al-Saif M, Al-Bakheet A, Hendrayani SF, Al-Yousef N, Kaya N, Khabar KS, and Aboussekhra A (2011). $p16^{INK4a}$ positively regulates cyclin D1 and E2F1 through negative control of AUF1. *PLoS One* **6**, e21111.

[39] Chien WW, Domenech C, Catallo R, Kaddar T, Magaud JP, Salles G, and Ffrench M (2011). Cyclin-dependent kinase 1 expression is inhibited by $p16^{INK4a}$ at the post-transcriptional level through the microRNA pathway. *Oncogene* **30**, 1880–1891.

[40] Holst CR, Nuovo GJ, Esteller M, Chew K, Baylin SB, Herman JG, and Tlsty TD (2003). Methylation of $p16^{INK4a}$ promoters occurs *in vivo* in histologically normal human mammary epithelia. *Cancer Res* **63**, 1596–1601.

[41] Crawford YG, Gauthier ML, Joubel A, Mantei K, Kozakiewicz K, Afshari CA, and Tlsty TD (2004). Histologically normal human mammary epithelia with silenced $p16^{INK4a}$ overexpress COX-2, promoting a premalignant program. *Cancer Cell* **5**, 263–273.